

Tool Building as a Path to “Superintelligence”

David Koplow Tomer Galanti Tomaso Poggio

February 25, 2026

Abstract

The *Diligent Learner* framework suggests LLMs can achieve superintelligence via test-time search, provided a sufficient step-success probability γ . In this work, we design a benchmark to measure γ on logical out-of-distribution inference. We construct a class of tasks involving GF(2) circuit reconstruction that grow more difficult with each reasoning step, and that are, from an information-theoretic standpoint, impossible to reliably solve unless the LLM carefully integrates all of the information provided. Our analysis demonstrates that while the γ value for small LLMs declines superlinearly as depth increases, frontier models exhibit partial robustness on this task. Furthermore, we find that successful reasoning at scale is contingent upon precise tool calls, identifying tool design as a critical capability for LLMs to achieve general superintelligence through the Diligent Learner framework.

1 Introduction

The recent emergence of large-scale LLMs has made multi-step reasoning increasingly practical Wei et al. (2022); Wang et al. (2022); Fu et al. (2023); Kojima et al. (2022), especially when combined with inference-time search, tool use, and verification. Much of this progress has been enabled by post-training, including reinforcement learning and preference-optimization methods Ouyang et al. (2022); Shao et al. (2024). Recent work on the *Diligent Learner*, suggests search through reasoning steps on problems of bounded depth could lead to “superintelligent” agents with our existing architectures (Shalev-Shwartz and Shashua, 2025b).

The viability of this framework hinges on a critical quantity: the stepwise success probability, denoted by γ . The central premise of Diligent Learning is that test-time search can scale effectively only if the model’s proposal distribution preserves a non-vanishing probability of generating the correct subsequent step. However, a central question remains unresolved; *as reasoning unfolds over longer horizons on tasks does the stepwise success probability γ always remain larger than a positive constant, or are there categories of problems for which it catastrophically degrades with depth?*

If a successful reasoning chain requires knowledge that the LLM has never been exposed to, then the answer is trivial. However, when it comes to the

problem of general superintelligence, the important question is whether or not the model can solve out-of-distribution problems while reasoning about prior learned relationships. In this work, we design a benchmark to measure exactly this quality.

While plenty of benchmarks exist for studying the reasoning capabilities of different models, existing evaluations are inadequate for this goal. Many benchmarks score only final answers, allow multiple valid intermediate paths, or permit shortcuts where performance comes from pattern-matching labeled data or memorizing prior examples. Thus, “stepwise reasoning” is confounded with exploiting benchmark-specific regularities and pre-trained knowledge.

To rigorously test the Diligent Learner hypothesis, we introduce a benchmark that is adversarial to such shortcuts. We design a form of Boolean circuit reconstruction from data over $\text{GF}(2)$. The model must predict successive terms in an Algebraic Normal Form (ANF) of the circuit. Each step g in the reasoning chain has a unique correct continuation. To find it, the model must combine two distinct inputs: (i) *The Prefix: The history of the circuit revealed so far* and (ii) *The Evidence: A new batch of step-specific data*.

To ensure that the model cannot cheat, we employ an *adversarial sampling oracle*. This oracle generates evidence that appears statistically random unless the solver conditions it on the prefix. Consequently, strategies that rely solely on pattern-matching of the data or memorizing of the history will fail. Only a diligent solver that integrates both sources can recover the next term.

We provide the models with a perfect oracle that prevents them from going down incorrect reasoning paths. This structure allows us to find an empirical upper-bound for γ_g and measure the affect of problem complexity and reasoning depth without need to fine-tune the model learn how to handle back-tracking.

When we apply this metric to current systems, we find that in smaller models, γ_g collapses as the reasoning depth increases. Frontier models, however, sustain a high γ_g over long horizons when using tool calls.

Contributions. Our main contributions are as follows:

- We formalize a step-by-step circuit reconstruction problem that enables testing of γ in the Diligent Learner framework.
- We build such a dataset and evaluate it on Bayesian estimators, small LLMs, and state-of-the-art LLMs.
- We identify trends in γ_g degradation and provide an analysis for why certain models seem to catastrophically fail as problem complexity increases, while some that use tool calls can perform far better.
- We release all code to reproduce our results and run further experiments on GitHub at: github.com/Poggio-Lab/Tool-Building-as-a-Path-to-Superintelligence.

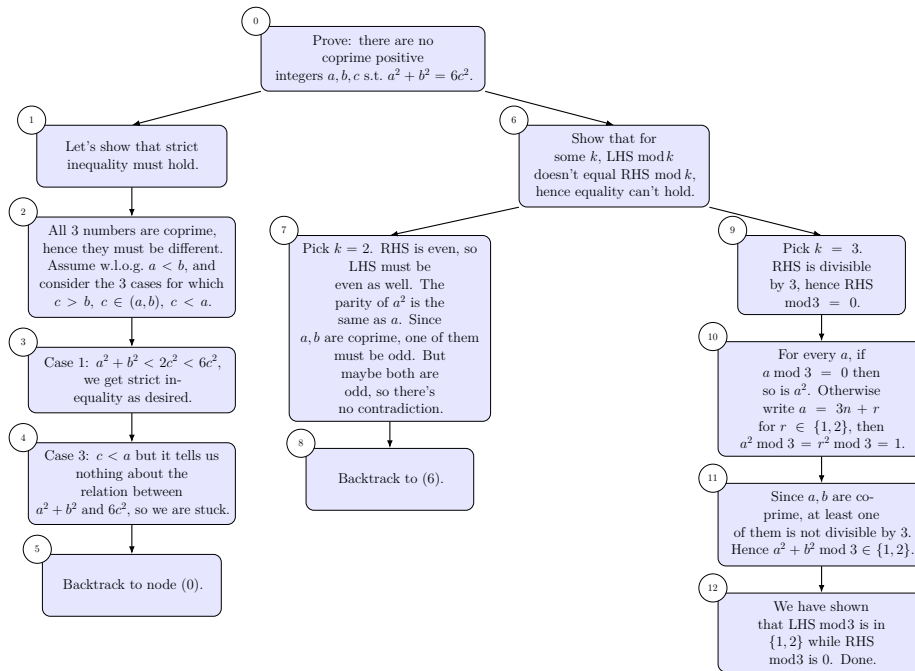


Figure 1: Diligent learner visualization from (Shalev-Shwartz and Shashua, 2025a).

2 Related Work

Reasoning as search with verification. A long line of work treats reasoning as a search problem where a model proposes candidate steps or solutions and an evaluation signal filters them; in LLMs, this appears in chain-of-thought prompting (Wei et al., 2022; Wang et al., 2022), Tree-of-Thought search over partial reasoning states (Yao et al., 2023), and iterative propose–critique–revise agentic loops such as Reflexion (Shinn et al., 2023). These approaches are often augmented with tool use (Schick et al., 2023; Hao et al., 2023; Parisi et al., 2022; Shi et al., 2025) and scratchpads (Nye et al., 2021) to maintain intermediate state and enable efficiently checkable substeps. On the theory side, chain-of-thought can be formalized as a task decomposition that makes otherwise hard concept classes learnable in a PAC-style setting (Yang et al., 2025a; Joshi et al., 2025), and next-token predictors can be viewed as general-purpose learners under suitable conditions (Malach, 2024). Closely related, the LLM-ERM framework treats the LLM as proposing hypotheses and a verifier as enforcing correctness (Singhal et al., 2025).

The Diligent Learner. Motivated by this broader view of reasoning as search guided by evaluation, a recent paper (Shalev-Shwartz and Shashua, 2025b) introduced the Diligent Learner framework in order to formalize the process

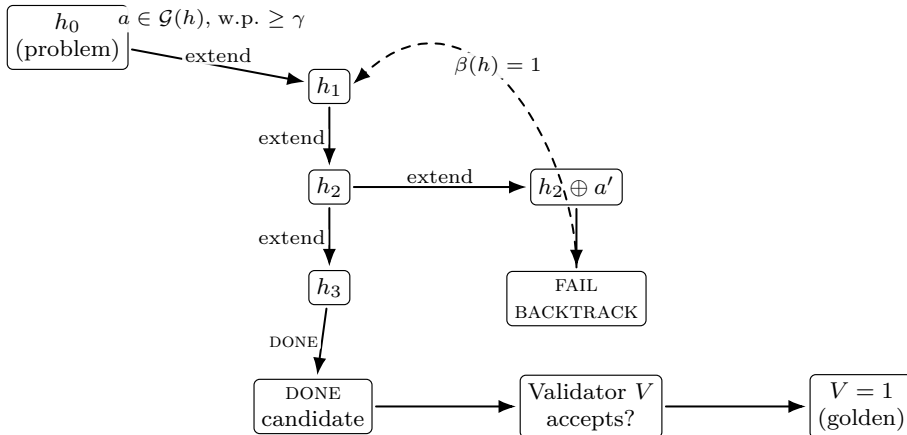


Figure 2: **Diligent Learner as validator-guided DFS.** Good extensions occur with probability at least γ . On failure, the policy backtracks to the deepest correct prefix $\beta(h)$ and continues search.

as validator-guided depth-first search with a BACKTRACK action. Its analysis isolates a single bottleneck, the per-step success probability γ , defined as the probability mass the policy assigns to “good” next steps that keep the current prefix completable. If γ does not collapse with depth and backtracking returns to the deepest correct prefix with high probability, search succeeds with controlled overhead (Shalev-Shwartz and Shashua, 2025b). Our work targets the empirical gap left open by this theory: γ is defined abstractly, but there is no standard benchmark in which (i) the correct extension is unique at each step and (ii) shortcuts that ignore either the accumulated history or the fresh evidence are information-theoretically ineffective. We design such a benchmark so that γ_g is directly measurable as exact-next accuracy at depth g .

Benchmarks for testing reasoning in LLMs. Reasoning in LLMs is commonly evaluated via static, single-shot benchmarks spanning mathematical and logical problem solving, including grade-school word problems and multi-step arithmetic (Cobbe et al., 2021), competition-style mathematics (Hendrycks et al., 2021), and curated hard subsets of broad capability suites (Suzgun et al., 2022). A complementary line of work uses synthetic or controlled-distribution tasks to probe compositional generalization and algorithmic structure, such as formal mathematical expression generation (Frieder et al., 2025) and software engineering benchmarks (Jimenez et al., 2024; Yang et al., 2025b). Finally, interactive evaluations target agentic reasoning with tools and environments, where success depends on multi-step planning and external actions (e.g., embodied or text-based worlds, or web interaction) (Shridhar et al., 2021; Zhou et al., 2024; Qin et al., 2024; Liu et al., 2025).

While these benchmarks are valuable for measuring end-to-end task performance, they typically (i) score only the final answer, (ii) admit many valid intermediate trajectories, and (iii) do not isolate whether success comes from

the evolving history, the current evidence, or dataset-specific shortcuts. In contrast, our goal is to operationalize the Diligent Learner’s per-step parameter γ in a setting where each depth g has a *unique* correct extension and where solvers that ignore either the revealed prefix or the fresh step-specific samples are information-theoretically ineffective. The stepwise GF(2) reconstruction benchmark we introduce is designed to meet these requirements, enabling direct measurement of γ_g as exact-next accuracy with a polynomial-time validator.

3 Background

3.1 The Diligent Learner

Reasoning as a search tree with validation. The Diligent Learner formalizes reasoning as building a rooted search tree whose root encodes the problem instance, and whose nodes represent *semantic* reasoning states (partial chains). A root-to-leaf path corresponds to a proposed chain-of-thought (CoT). Leaves have two special types: DONE (a completed solution) and BACKTRACK (indicating a jump to an earlier node). A *validator* V checks a proposed step could logically follow from a prior one; a *golden path* is a root-to-DONE path accepted by V (see Figure 1).

Generator policy and step-success probability. Let V be a validator on the proposed next step. Let $\pi_\theta(\cdot | h, V)$ be a stochastic policy over valid actions given a partial reasoning state h (a prefix of a path). An *extension* action a proposes the next semantic step and S is a function that returns true if there exists a path to the conclusion of a reasoning problem given the prefix (h, a) .

$$\Pr_{a \sim \pi_\theta(\cdot | h)} [a \in \{\forall a_i. S(h, a_i) = 1\}] \geq \gamma. \tag{1}$$

Intuitively, γ is the probability mass assigned to *useful* next moves that keep the trace completable.

Learned backtracking. The original diligent learner allows the model to make incorrect extensions so long as it is able to realize and revert via depth-first-search. However, in this paper we assume a very strong validator that prevents the model from going down incorrect paths so we never need to fine-tune the model to learn how to back-track.

The implications of γ . If the policy keeps a nontrivial chance γ of proposing a good next step and can backtrack to the last correct prefix, then depth-first search reaches a validator-accepted leaf with high probability without exponential blowup. Concretely, for a target failure probability δ and maximum depth T_{\max} , the analysis sets

$$O\left(T_{\max} \cdot \frac{\log(T_{\max}/\delta)}{\gamma}\right) \tag{2}$$

which is polynomial in T_{\max} for constant γ (Shalev-Shwartz and Shashua, 2025b). Thus, the central requirement is that γ not decay with depth; otherwise the search budget grows rapidly and the guarantee becomes vacuous.

4 Theory

The ‘‘Diligent Learner’’ hypothesis posits that a reasoning model can solve long multi-step problems by performing test-time search, as long as it maintains a non-vanishing probability γ of proposing a *good* next semantic step at every depth (Shalev-Shwartz and Shashua, 2025b). We introduce a stepwise reconstruction benchmark to evaluate the limitations of this framework in which, at each step g , the model must extend a revealed partial solution (the current prefix) using a new batch of evidence specific to that step. The construction is designed to eliminate two shortcut strategies: (i) *data-only* prediction that ignores the prefix and tries to infer the next step from examples alone, and (ii) *history-only* prediction that ignores the new evidence and extrapolates from the prefix alone.

4.1 Problem formulation

We instantiate this in the reconstruction of Boolean functions over $\text{GF}(2)$ under a fixed-prefix statistical obfuscation sampling oracle.

Targets in ANF over $\text{GF}(2)$. Let $x = (a, v) \in \{0, 1\}^{n+p}$ where $a = (a_1, \dots, a_n) \in \{0, 1\}^n$ are *address bits* and $v = (v_1, \dots, v_p) \in \{0, 1\}^p$ are *payload bits*. We consider Boolean targets represented in Algebraic Normal Form (ANF) as XORs of monomials $f(a, v) = \bigoplus_{j=1}^n t_j(a, v)$, where

$$t_j(a, v) := a_j M_j(v), \quad M_j(v) := \prod_{i \in S_j} v_i, \quad (3)$$

such that each support $S_j \subseteq [p]$ has fixed size $|S_j| = d - 1$. Thus each term has payload-degree $d - 1$ and total degree d in (a, v) . An *instance* is specified by the ordered sequence of supports (S_1, \dots, S_n) (equivalently, the ordered ANF terms (t_1, \dots, t_n)), sampled once and then fixed.

Stepwise reconstruction game and step-success. At step $g \in \{0, \dots, n - 1\}$ the learner is given (i) the ordered prefix $P_g := (t_1, \dots, t_g)$ and (ii) a fresh labeled sample set $S_g := \{(x^{(k)}, y^{(k)})\}_{k=1}^K$ generated by the step- g oracle. The learner outputs a candidate monomial \hat{t} and succeeds iff $\hat{t} = t_{g+1}$. We define the benchmark step-success probability:

$$\gamma_g := \Pr_{\hat{t} \sim \pi_\theta(\cdot | P_g, S_g)} [\hat{t} = t_{g+1}], \quad (4)$$

where the probability is over instance generation, oracle sampling, and model stochasticity. Because the instance commits to an ordered sequence, at depth g there is a unique correct extension t_{g+1} , so γ_g directly operationalizes step-success in our benchmark.

Estimator classes. We distinguish solvers by their information access: (i) **Diligent Estimator** (\mathcal{A}_g): access to (P_g, S_g) ; (ii) **Data-only Estimator** (\mathcal{B}_g): access to S_g but not P_g ; (iii) **History-only Estimator** (\mathcal{C}_g): access to P_g but not S_g ; (iv) **Partial Estimator** (\mathcal{D}_g): partial access to P_g and S_g . Let $\gamma_g^{\mathcal{X}}$ denote the exact-next success probability for class \mathcal{X} at step g . Our benchmark

is designed to enforce a separation of the form

$$\min_g \gamma_g^A \geq Q \quad \text{while} \quad \gamma_g^B, \gamma_g^C, \gamma_g^D \approx \frac{1}{\binom{p}{d-1}}. \quad (5)$$

for a nontrivial constant $1 \geq Q \gg 0$.

4.2 Statistical Obfuscation: Construction and Guarantees

Theoretical Objectives. The primary goal of our benchmark is to defeat reasoning strategies that take shortcuts to ensure that problem complexity scales predictably as depth increases. To achieve this, we design a *statistical obfuscation sampling oracle*. Think of the revealed history as a cryptographic key. The oracle uses this key to unmask the labels of the step-specific data. For this benchmark to achieve this goal, our construction must satisfy three theoretical guarantees:

1. *No History-Only Shortcuts:* Knowing the sequence of prior steps must provide zero predictive power about the *next* step when not accounting for the new data.
2. *No Statistical Leakage:* The labels of the dataset must not be heavily biased towards 0 or 1; otherwise, a model could trivially guess the answer without reasoning.
3. *No Data-Only Shortcuts:* Looking at the new data without the history must provide negligible information.

Below, we detail the construction of our instances and oracle, proving how each component satisfies these three objectives.

Instance Generation. We first generate the underlying *instance*. We sample an ordered sequence of payload supports $S_1, \dots, S_n \subseteq [p]$ with $|S_j| = d-1$ once per instance. This fixes the ordered Algebraic Normal Form (ANF) terms (t_1, \dots, t_n) in (3).

Because the sequence of supports is sampled independently, the history prefix provides no mutual information about the upcoming support. This guarantees that history-only solvers fail.

Lemma 4.1 (History-only is prior guessing). *Assume the instance distribution samples supports S_1, \dots, S_n i.i.d. uniformly (with replacement) from $\{S \subseteq [p] : |S| = d-1\}$. Then for any $g < n$, conditioned on the revealed prefix P_g , the next support S_{g+1} is uniform over $\{S \subseteq [p] : |S| = d-1\}$ and independent of P_g . Consequently, any history-only estimator satisfies $\Pr[\hat{S} = S_{g+1}] \leq \frac{1}{\binom{p}{d-1}}$.*

Payload Distribution. Next, we define the *payload distribution* to ensure our evaluations have no trivial statistical leakage. We fix a Hamming weight w and sample payloads uniformly from the sphere $\{v \in \{0, 1\}^p : \|v\|_0 = w\}$. Because we draw payloads uniformly from a fixed Hamming sphere, the probability that a monomial fires admits a simple closed form.

Lemma 4.2 (Monomial firing probability at fixed Hamming weight). *Fix integers $p \geq d - 1 \geq 1$ and $w \in \{0, \dots, p\}$. Let v be uniform over the Hamming sphere $\{v \in \{0, 1\}^p : \|v\|_0 = w\}$, and fix any $S \subseteq [p]$ with $|S| = d - 1$. Define $M_S(v) := \prod_{i \in S} v_i$. Then*

$$\Pr [M_S(v) = 1] = \begin{cases} \frac{\binom{w}{d-1}}{\binom{p}{d-1}} = \frac{\binom{p-(d-1)}{w-(d-1)}}{\binom{p}{w}} & \text{if } w \geq d - 1, \\ 0 & \text{if } w < d - 1. \end{cases}$$

Let $\rho(w) := \Pr [M_S(v) = 1]$. We intentionally choose a specific weight w^* to make $\rho(w)$ as close to $1/2$ as possible. This ensures that the monomial evaluations are nearly balanced in expectation, eliminating bias shortcuts.

Obfuscation Sampling. Finally, we define the *step- g sampling oracle*. Given an instance and depth $g \in \{0, \dots, n - 1\}$, the oracle returns a fresh labeled set $S_g = \{(a^{(k)}, v^{(k)}, y^{(k)})\}_{k=1}^K$ by sampling i.i.d. examples as follows: (i) Set the target address bit $a_{g+1} = 1$ and set all future bits $a_j = 0$ for all $j > g + 1$; (ii) Sample the prefix address bits $a_1, \dots, a_g \stackrel{i.i.d.}{\sim} \text{Bernoulli}(1/2)$; (iii) Sample the payload v uniformly from $\{v : \|v\|_0 = w^*\}$; (iv) Output the label $y := f(a, v)$.

Because $a_{g+1} = 1$ and all subsequent address bits are 0, the resulting label naturally decomposes into a mask and a signal:

$$y = \underbrace{\left(\bigoplus_{j=1}^g a_j M_j(v) \right)}_{\text{prefix obfuscation}} \oplus \underbrace{M_{g+1}(v)}_{\text{next-term signal}}. \quad (6)$$

This mask is computable from the prefix (P_g, x) , allowing a diligent solver to recover the signal. However, to a data-only estimator lacking the prefix, the mask functions as a high-entropy statistical obfuscator. By marginalizing over the unknown prefix supports, we prove that the Bayes advantage from any single sample shrinks exponentially with the number of active prefix bits.

Lemma 4.3 (Bayes masking given observed (a, v)). *Assume the instance distribution samples S_1, \dots, S_g, S_{g+1} i.i.d. uniformly from $\{S \subseteq [p] : |S| = d - 1\}$, independently of the oracle samples. Fix a step g and condition on a realized example (a, v) with $\|v\|_0 = w^*$. Let*

$$\rho := \rho(w^*) = \Pr_S [M_S(v) = 1] = \frac{\binom{w^*}{d-1}}{\binom{p}{d-1}}, \quad m := m(a).$$

Then, marginalizing over the unknown prefix supports (S_1, \dots, S_g) , for each $r \in \{0, 1\}$,

$$\Pr [B(a, v) = r \mid a, v] = \frac{1}{2} [1 + (-1)^r (1 - 2\rho)^m].$$

Moreover, $B(a, v)$ is independent of $b = M_{g+1}(v)$ given (a, v) , and since $y = B(a, v) \oplus b$ we have

$$|\Pr [y = b \mid a, v] - \frac{1}{2}| = \frac{1}{2} |1 - 2\rho|^m.$$

Under our oracle, $a_1, \dots, a_g \stackrel{i.i.d.}{\sim} \text{Bernoulli}(1/2)$, so a typical example has $m \approx g/2$ active prefix bits. Therefore, when ρ is close to $1/2$, a typical sample provides essentially zero information about the signal b without the revealed prefix.

Recoverability in polynomial time for diligent solvers. See Appendix B.

5 The Benchmark

While Section 4 establishes the information-theoretic properties of our statistical obfuscation, this section details its instantiation as a benchmark. We procedurally generate instances to evaluate an LLM’s *reasoning horizon*.

5.1 Prompt Structure

To test LLMs we must convert the theoretical construction into a prompt that the model can understand. To isolate a model’s ability to integrate state with new evidence, we format the evaluation as a single-turn completion prompt. We flatten the bipartite variables into a unified sequence x_0, x_1, \dots, x_{N-1} and define the target circuit as the XOR sum of monomials ($y = M_1 \oplus M_2 \cdots \oplus M_{g+1}$). At step g , the prompt provides:

1. **Global Metadata:** The total number of variables N and the expected degree of the target monomial.
2. **The Prefix (P_g):** The sequence of g previously discovered Algebraic Normal Form (ANF) terms. To minimize format-induced errors, these are presented as logical conjunctions over the variable space.
3. **The Evidence (S_g):** A tabular presentation of 32 labeled, step-specific observations. To prevent tokenization artifacts, the N -bit inputs are formatted as space-separated binary strings, paired with their corresponding binary outputs y .

Importantly, we do not require the model to blindly deduce the bipartite structure. The prompt also identifies the active address variable for the current step (x_g) and provides the valid partition boundary n . The model is instructed to search strictly within the payload index range $[n, N - 1]$ to find the remaining $d - 1$ variables that complete the unknown monomial M_{g+1} .

To succeed, the model must apply the prefix to the new evidence to cancel the obfuscation mask and isolate the signal within the specified search space. It must then output the indices of the discovered payloads.

Although we direct the model to answer using a particular notation, it frequently fails to adhere to this format. To handle this, we use a sophisticated regex-based parser that compensates for many typical syntactic errors and still accepts an answer as correct as long as the supplied indices are right, even if the overall format is not.

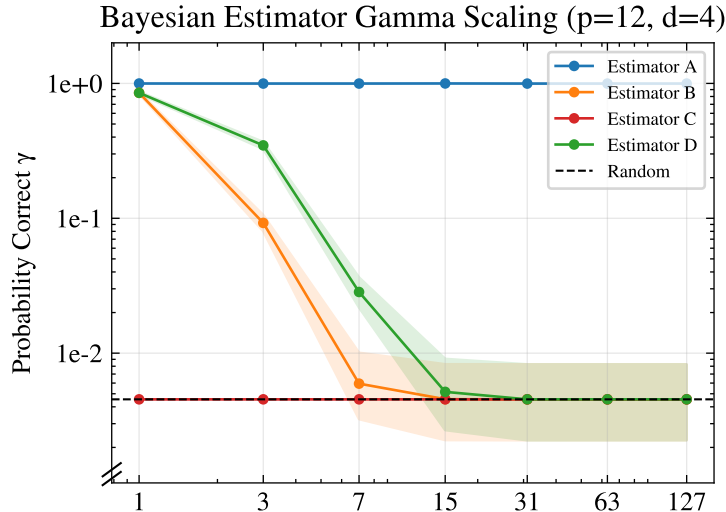


Figure 3: Only history and data sustains reliable next-step prediction. Step success γ_g (probability mass on the correct next monomial) versus depth g for each estimator class. Curves show the mean over 2000 generated circuits per depth, with shaded Jeffreys intervals. The diligent estimator \mathcal{A} (history+data) maintains high γ_g across depths, whereas \mathcal{B} (data-only) and \mathcal{D} (partial) frequently collapse toward zero mass, and \mathcal{C} (history-only) remains at chance.

5.2 Validation and Evaluation

A primary bottleneck in evaluating multi-step logical reasoning is the computational cost of intermediate verification. Determining whether a proposed intermediate circuit state can still lead to a valid final solution typically requires super-exponential time in the number of gates.

Our construction completely avoids this limitation. Because the instance generator adheres to a deterministic curriculum and the oracle adaptively masks all future terms, there is exactly one valid continuation at each step g . As a result, validation reduces to parsing the model’s boxed array and checking set equivalence with the withheld ground-truth indices. For a monomial of degree d , this validation procedure runs in $O(d)$ time. Since d is a small constant, the validation cost is negligible.

To estimate the step-success parameter γ from the Diligent Learner framework, we measure the exact-match accuracy γ_g across varying reasoning depths, evaluated at exponential intervals ($g = 2^k - 1$). By tracking γ_g as g increases, we directly quantify how proposal quality scales with problem complexity, identifying the precise horizon at which a model’s state-tracking capabilities degrade.

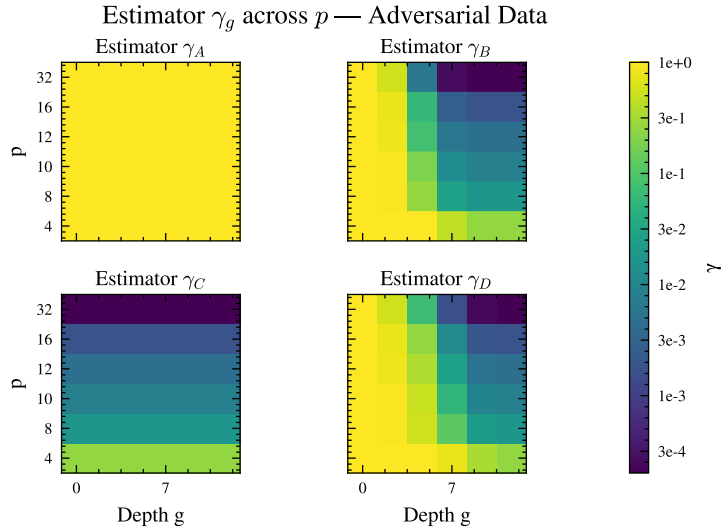


Figure 4: As both g and p increase, the probability of an estimator with imperfect information begins to collapse to zero. Only Estimator \mathcal{A} is able to consistently produce the next monomial. The above heatmap was constructed through generating 200 circuits for each combination of hyperparameters and computing the corresponding γ_g for each p .

6 Results

We evaluated the four estimators described in Sec. 3.1, small LLMs, and frontier models to analyze empirically how gamma changes with depth.

6.1 Estimator Simulations

We evaluated small LLMs to test whether they exhibit the same depth-induced degradation in next-step prediction as estimator \mathcal{D} . As shown in Figure 5, all models display a systematic decline in γ_g with depth, even though a polynomial-time decoder exists at every step (Thm. B.1). Larger models and “thinking” variants perform better at shallow depths, but depth sensitivity persists.

We consider four models from the Qwen3-2507 family: **4B-Instruct**, **4B-Thinking**, **30B-A3B-Thinking**, and **30B-A3B-Instruct** (Team, 2025). We run inference in vLLM on 3000 generated instances, evenly split across $g \in \{1, 3, 7, 15, 31\}$, using adversarial sampling with $p = 12$ and $d = 4$ (Kwon et al., 2023). **4B-Instruct** does not achieve performance statistically distinguishable from random guessing even at the easiest setting, so we omit it for readability. **Qwen3-30B-A3B-Thinking** has a clear advantage at small depths over its instruct variant, but still drops sharply at intermediate depths (around $g=15$ here) and approaches the trivial baseline γ_{triv} .

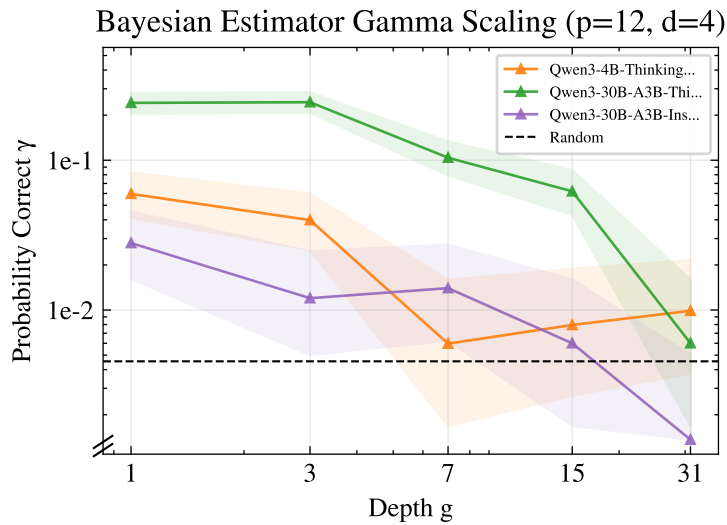


Figure 5: Small LLMs exhibit depth-induced collapse in next-step prediction. Step-success γ_g (probability mass on the correct next monomial) versus circuit depth g for Qwen3-2507 models under adversarial sampling ($p = 12, d = 4$). Despite the existence of a polynomial-time decoder at every step (Thm. B.1), all models degrade with depth: larger and “thinking” variants help at small g , but performance drops sharply at intermediate depths and approaches the trivial baseline γ_{triv} , indicating limited ability to maintain the prefix-conditioned cancellation required for continued progress.

6.2 Small LLMs

We evaluated small LLMs to test whether they exhibit the same depth-induced degradation in next-step prediction as estimator \mathcal{D} . As shown in Figure 5, all models display a systematic decline in γ_g with depth, qualitatively mirroring the collapse seen for partial-information estimators, even though a polynomial-time decoder exists at every step (Thm. B.1). Larger models and “thinking” variants perform better at shallow depths, but depth sensitivity persists.

We consider four models from the Qwen3-2507 family: **4B-Instruct**, **4B-Thinking**, **30B-A3B-Thinking**, and **30B-A3B-Instruct**. We run inference in vLLM on 3000 generated instances, evenly split across $g \in \{1, 3, 7, 15, 31\}$, using adversarial sampling with $p = 12$ and $d = 4$. This task requires long contexts for consistent decoding (max context length 32,768 for 4B and 81,920 for 30B). **4B-Instruct** does not achieve performance statistically distinguishable from random guessing even at the easiest setting, so we omit it for readability. **Qwen3-30B-A3B-Thinking** has a clear advantage at small depths over its instruct variant, but still drops sharply at intermediate depths (around $g=15$ here) and approaches the trivial baseline γ_{triv} .

Effective-prefix analysis (linking to partial-information estimators). To connect these empirical trends to the “partial access” thread (Sec. 4.1), we fit each model’s accuracy curve to an effective-prefix abstraction: performance at depth g is modeled as if the solver only uses k of the g revealed terms, with either proportional scaling $k = ug$ or constant capacity $k = v$. Table 1 shows strong evidence that **Qwen3-30B-A3B-Thinking** behaves like it uses a constant fraction of the revealed prefix ($u \approx 0.77$), whereas **Qwen3-30B-A3B-Instruct** exhibits only weak scaling ($u \approx 0.15$). The 4B models do not meaningfully distinguish proportional and constant-capacity fits. This data suggests that as g grows, the oracle mask involves an expanding set of prefix monomials, and limited effective prefix utilization pushes models toward the partial-information regime.

6.3 Frontier LLMs

We now extend our analysis of depth-induced collapse in small models to larger systems: GPT 5.2 with extended Thinking, Claude Opus 4.5 with max Thinking, and Gemini 3 Pro (Jan 2026). Because frontier models typically generate extremely long reasoning traces on this task, it was financially prohibitive to replicate the full experimental protocol from Section 6.2. Nonetheless, the findings in the previous section provide a strong prior that guides our interpretation of the observed trends in γ_g for these larger models, even with fewer data points. In this section, we report results from 60 queries per model, spread across $g \in \{31, 63, 127\}$ with $p = 12$ and $d = 4$. For half of the prompts, the model was instructed not to use tool calls; for the other half, it was free to choose any solution strategy, including tool use.

Frontier models are significantly better. Under the hardest conditions shown in 5, at which all small LLMs perform at random on the task, frontier models are still able to solve each step with a very high probability (Figure 6).

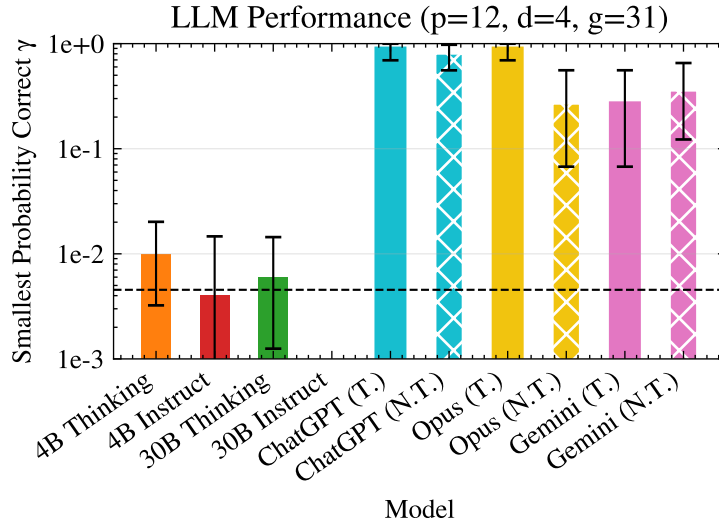


Figure 6: Frontier LLMs have a much higher γ_g than the smaller LLMs we tried.

Tools stabilize γ_g over long horizons. Tool-enabled models maintain near-unity γ_g even at $g=127$, far exceeding the trivial baseline γ_{triv} (Figure 7).

These results offer a clear perspective on the Diligent Learner framework and on multi-step reasoning more broadly. Each reasoning step involves two distinct requirements: inferring the correct constraints from the available inputs and data, and executing the computation implied by those constraints. Failure at either stage causes the reasoning chain to break.

Tool use fundamentally alters this dynamic. By externalizing execution, tools allow the model to focus primarily on specifying constraints rather than simultaneously discovering and implementing the full computation. This separation is critical for generalization. Prior work on LLM generalization suggests that, absent tools, success on out-of-distribution reasoning requires sparse compositional structure within the model’s parameters, enabling both the representation of constraints and the implicit execution of the induced algorithm. This places a strong burden on the transformer’s internal weights.

When tools are available, the model instead communicates constraints and delegates execution to an external program. This results in a much sparser effective algorithm at each step, which substantially improves generalization and stabilizes stepwise success probability. This mechanism explains why all tool-using models exhibit dramatically higher and more stable γ_g than their no-tool counterparts.

Tool-based reasoning remains imperfect, however, as it still relies on copying intermediate data through context. A natural extension would allow models to apply learned programs directly to their inputs, avoiding this degradation. Notably, the only model to perform well “without” tool use was Opus, but

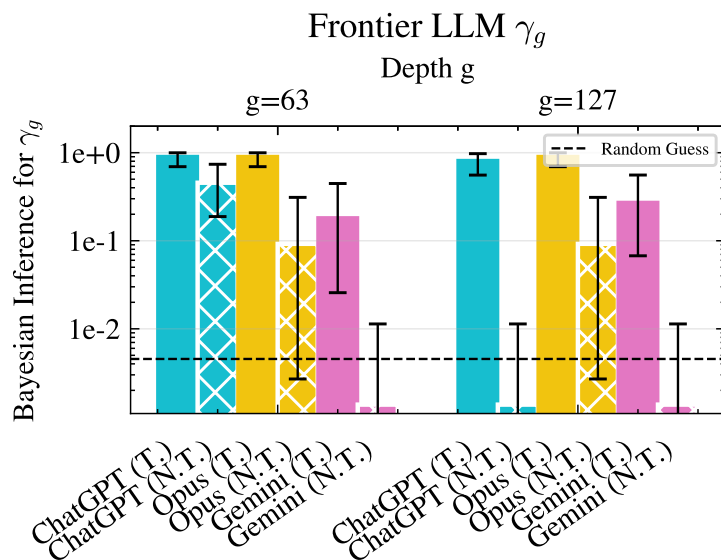


Figure 7: Frontier models that use tool calls (denoted with T.) have a much larger γ_g for this task and see minimal degradation, even at very significant model depths. When models are instructed not to use tools (denoted by N.T.), performance drops substantially as problem size increases. Opus often still used tool calls even when instructed not to, leading to inflation of its no-tools score, though it was challenging to determine exactly which instances used tools. The bars show the Bayesian confidence interval with a random prior as supported by the results in Section 6.2.

closer inspection suggests that it frequently invoked tool-like behavior despite instructions to the contrary, though such usage was not always transparent.

7 Discussion

In this work, we offer a rigorous empirical test of the *Diligent Learner* hypothesis by introducing a GF(2) circuit reconstruction benchmark that is adversarial to common shortcut strategies. The task forces a model to maintain state and repeatedly fuse accumulated historical context with newly observed evidence at every step, rather than relying on shallow pattern matching. Across this benchmark, we observe a clear divide in behavior: smaller language models exhibit a superlinear decline in γ as problem depth increases, effectively acting as partial-information estimators that cannot preserve the needed state. In contrast, frontier models that leverage tools maintain high γ over long sequences by delegating state tracking and verification to external mechanisms. Within the Diligent Learner framework, this suggests that progress toward “superintelligence” depends less on scaling test-time compute or deepening search, and more on architectures that can build and use tools.

References

- Karl Cobbe, Vineet Kosaraju, Mohammad Bavarian, Mark Chen, Heewoo Jun, Lukasz Kaiser, Matthias Plappert, Jerry Tworek, Jacob Hilton, Reiichiro Nakano, Christopher Hesse, and John Schulman. Training verifiers to solve math word problems, 2021. URL <https://arxiv.org/abs/2110.14168>.
- Simon Frieder, Jonas Bayer, Sam Looi, Jacob Loader, Julius Berner, Katherine M. Collins, András Juhász, Fabian Ruehle, Sean Welleck, Gabriel Poesia, Ryan-Rhys Griffiths, Adrian Weller, Anirudh Goyal, Cameron Freer, Thomas Lukasiewicz, and Timothy Gowers. Data for mathematical copilots: Better ways of presenting proofs for machine learning, 2025. URL <https://arxiv.org/abs/2412.15184>.
- Yao Fu, Hao Peng, Litu Ou, Ashish Sabharwal, and Tushar Khot. Specializing smaller language models towards multi-step reasoning. In Andreas Krause, Emma Brunskill, Kyunghyun Cho, Barbara Engelhardt, Sivan Sabato, and Jonathan Scarlett, editors, *Proceedings of the 40th International Conference on Machine Learning*, volume 202 of *Proceedings of Machine Learning Research*, pages 10421–10430. PMLR, 23–29 Jul 2023. URL <https://proceedings.mlr.press/v202/fu23d.html>.
- John Garrett, Echedey Luis, H.-H. Peng, Tim Cera, gobinathj, Josh Borrow, Mehmet Keçeci, Splines, Suraj Iyer, Yuming Liu, cju, and Mikhail Gasanov. garrettj403/scienceplots: 2.1.1, November 2023. URL <https://zenodo.org/records/10206719>.

- Shibo Hao, Tianyang Liu, Zhen Wang, and Zhiting Hu. ToolkenGPT: Augmenting frozen language models with massive tools via tool embeddings. In *Thirty-seventh Conference on Neural Information Processing Systems*, 2023. URL <https://openreview.net/forum?id=BHXsb69bSx>.
- Dan Hendrycks, Collin Burns, Steven Basart, Andy Zou, Mantas Mazeika, Dawn Song, and Jacob Steinhardt. Measuring massive multitask language understanding. In *International Conference on Learning Representations*, 2021. URL <https://openreview.net/forum?id=d7KBjmI3GmQ>.
- Carlos E Jimenez, John Yang, Alexander Wettig, Shunyu Yao, Kexin Pei, Ofir Press, and Karthik R Narasimhan. SWE-bench: Can language models resolve real-world github issues? In *The Twelfth International Conference on Learning Representations*, 2024. URL <https://openreview.net/forum?id=VTF8yNQM66>.
- Nirmit Joshi, Gal Vardi, Adam Block, Surbhi Goel, Zhiyuan Li, Theodor Misiakiewicz, and Nathan Srebro. A theory of learning with autoregressive chain of thought, 2025. URL <https://arxiv.org/abs/2503.07932>.
- Takeshi Kojima, Shixiang Shane Gu, Machel Reid, Yutaka Matsuo, and Yusuke Iwasawa. Large language models are zero-shot reasoners. In *Proceedings of the 36th International Conference on Neural Information Processing Systems, NIPS '22*, Red Hook, NY, USA, 2022. Curran Associates Inc. ISBN 9781713871088.
- Woosuk Kwon, Zhuohan Li, Siyuan Zhuang, Ying Sheng, Lianmin Zheng, Cody Hao Yu, Joseph E. Gonzalez, Hao Zhang, and Ion Stoica. Efficient memory management for large language model serving with pagedattention. In *Proceedings of the ACM SIGOPS 29th Symposium on Operating Systems Principles (SOSP '23)*, 2023. doi: 10.1145/3600006.3613165.
- Xiao Liu, Hao Yu, Hanchen Zhang, Yifan Xu, Xuanyu Lei, Hanyu Lai, Yu Gu, Hangliang Ding, Kaiwen Men, Kejuan Yang, Shudan Zhang, Xiang Deng, Aohan Zeng, Zhengxiao Du, Chenhui Zhang, Sheng Shen, Tianjun Zhang, Yu Su, Huan Sun, Minlie Huang, Yuxiao Dong, and Jie Tang. Agentbench: Evaluating llms as agents, 2025. URL <https://arxiv.org/abs/2308.03688>.
- Eran Malach. Auto-regressive next-token predictors are universal learners. In *Proceedings of the 41st International Conference on Machine Learning, ICML'24*. JMLR.org, 2024.
- Maxwell Nye, Anders Johan Andreassen, Guy Gur-Ari, Henryk Michalewski, Jacob Austin, David Bieber, David Dohan, Aitor Lewkowycz, Maarten Bosma, David Luan, Charles Sutton, and Augustus Odena. Show your work: Scratchpads for intermediate computation with language models, 2021. URL <https://arxiv.org/abs/2112.00114>.

- Long Ouyang, Jeff Wu, Xu Jiang, Diogo Almeida, Carroll L. Wainwright, Pamela Mishkin, Chong Zhang, Sandhini Agarwal, Katarina Slama, Alex Ray, John Schulman, Jacob Hilton, Fraser Kelton, Luke Miller, Maddie Simens, Amanda Askell, Peter Welinder, Paul Christiano, Jan Leike, and Ryan Lowe. Training language models to follow instructions with human feedback. In *Proceedings of the 36th International Conference on Neural Information Processing Systems*, NIPS '22, Red Hook, NY, USA, 2022. Curran Associates Inc. ISBN 9781713871088.
- Aaron Parisi, Yao Zhao, and Noah Fiedel. Talm: Tool augmented language models, 2022. URL <https://arxiv.org/abs/2205.12255>.
- Yujia Qin, Shihao Liang, Yining Ye, Kunlun Zhu, Lan Yan, Yaxi Lu, Yankai Lin, Xin Cong, Xiangru Tang, Bill Qian, Sihan Zhao, Lauren Hong, Runchu Tian, Ruobing Xie, Jie Zhou, Mark Gerstein, dahai li, Zhiyuan Liu, and Maosong Sun. ToolLLM: Facilitating large language models to master 16000+ real-world APIs. In *The Twelfth International Conference on Learning Representations*, 2024. URL <https://openreview.net/forum?id=dHng200Jjr>.
- Timo Schick, Jane Dwivedi-Yu, Roberto Dessi, Roberta Raileanu, Maria Lomeli, Eric Hambro, Luke Zettlemoyer, Nicola Cancedda, and Thomas Scialom. Toolformer: Language models can teach themselves to use tools. In *Thirty-seventh Conference on Neural Information Processing Systems*, 2023. URL <https://openreview.net/forum?id=Yacmpz84TH>.
- Shai Shalev-Shwartz and Amnon Shashua. From reasoning to super-intelligence: A search-theoretic perspective. *arXiv preprint arXiv:2507.15865*, 2025a. URL <https://arxiv.org/abs/2507.15865>.
- Shai Shalev-Shwartz and Amnon Shashua. From reasoning to super-intelligence: A search-theoretic perspective. *arXiv preprint arXiv:2507.15865*, 2025b.
- Zhihong Shao, Peiyi Wang, Qihao Zhu, Runxin Xu, Junxiao Song, Xiao Bi, Haowei Zhang, Mingchuan Zhang, Y. K. Li, Y. Wu, and Daya Guo. Deepseek-math: Pushing the limits of mathematical reasoning in open language models, 2024. URL <https://arxiv.org/abs/2402.03300>.
- Zhengliang Shi, Shen Gao, Lingyong Yan, Yue Feng, Xiuyi Chen, Zhumin Chen, Dawei Yin, Suzan Verberne, and Zhaochun Ren. Tool learning in the wild: Empowering language models as automatic tool agents. In *Proceedings of the ACM on Web Conference 2025*, WWW '25, page 2222–2237, New York, NY, USA, 2025. Association for Computing Machinery. ISBN 9798400712746. doi: 10.1145/3696410.3714825. URL <https://doi.org/10.1145/3696410.3714825>.
- Noah Shinn, Federico Cassano, Edward Berman, Ashwin Gopinath, Karthik Narasimhan, and Shunyu Yao. Reflexion: Language agents with verbal reinforcement learning. *arXiv preprint arXiv:2303.11366*, 2023. doi: 10.48550/arXiv.2303.11366. URL <https://arxiv.org/abs/2303.11366>.

- Mohit Shridhar, Xingdi Yuan, Marc-Alexandre Côté, Yonatan Bisk, Adam Trischler, and Matthew Hausknecht. ALFWorld: Aligning Text and Embodied Environments for Interactive Learning. In *Proceedings of the International Conference on Learning Representations (ICLR)*, 2021. URL <https://arxiv.org/abs/2010.03768>.
- Shivam Singh, Eran Malach, Tomaso Poggio, and Tomer Galanti. LLM-ERM: A probabilistic framework for in-context learning and text generation. *arXiv preprint arXiv:2510.14331*, 2025.
- Mirac Suzgun, Nathan Scales, Nathanael Schärli, Sebastian Gehrmann, Yi Tay, Hyung Won Chung, Aakanksha Chowdhery, Quoc V. Le, Ed H. Chi, Denny Zhou, and Jason Wei. Challenging big-bench tasks and whether chain-of-thought can solve them, 2022. URL <https://arxiv.org/abs/2210.09261>.
- Qwen Team. Qwen3 technical report, 2025. URL <https://arxiv.org/abs/2505.09388>.
- Xuezhi Wang, Jason Wei, Dale Schuurmans, Quoc V. Le, Ed H. Chi, Sharan Narang, Aakanksha Chowdhery, and Denny Zhou. Self-consistency improves chain of thought reasoning in language models. *arXiv preprint arXiv:2203.11171*, 2022. URL <https://arxiv.org/abs/2203.11171>.
- Jason Wei, Xuezhi Wang, Dale Schuurmans, Maarten Bosma, Brian Ichter, Fei Xia, Ed H. Chi, Quoc V. Le, and Denny Zhou. Chain-of-thought prompting elicits reasoning in large language models. *arXiv preprint arXiv:2201.11903*, 2022. doi: 10.48550/arXiv.2201.11903. URL <https://arxiv.org/abs/2201.11903>.
- Chenxiao Yang, Zhiyuan Li, and David Wipf. Chain-of-thought provably enables learning the (otherwise) unlearnable. In *The Thirteenth International Conference on Learning Representations*, 2025a. URL <https://openreview.net/forum?id=N6pbLYLeej>.
- John Yang, Carlos E Jimenez, Alex L Zhang, Kilian Lieret, Joyce Yang, Xindi Wu, Ori Press, Niklas Muennighoff, Gabriel Synnaeve, Karthik R Narasimhan, Diyi Yang, Sida Wang, and Ofir Press. SWE-bench multimodal: Do AI systems generalize to visual software domains? In *The Thirteenth International Conference on Learning Representations*, 2025b. URL <https://openreview.net/forum?id=riTiq3i21b>.
- Shunyu Yao, Dian Yu, Jeffrey Zhao, Izhak Shafran, Thomas L. Griffiths, Yuan Cao, and Karthik Narasimhan. Tree of thoughts: Deliberate problem solving with large language models. *arXiv preprint arXiv:2305.10601*, 2023. URL <https://arxiv.org/abs/2305.10601>.
- Shuyan Zhou, Frank F. Xu, Hao Zhu, Xuhui Zhou, Robert Lo, Abishek Sridhar, Xianyi Cheng, Tianyue Ou, Yonatan Bisk, Daniel Fried, Uri Alon, and Graham Neubig. Webarena: A realistic web environment for building autonomous agents, 2024. URL <https://arxiv.org/abs/2307.13854>.

A Other Simulations

See Figures 8 and 9, as well as Table 1.

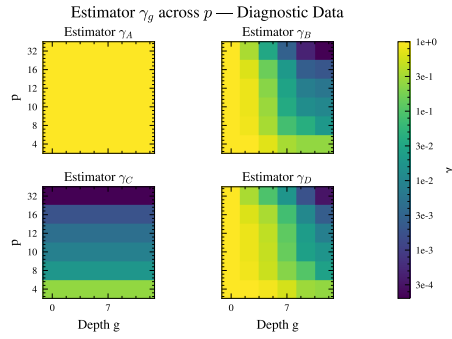


Figure 8: As both g and p increase, the probability of an estimator with imperfect information begins to collapse to zero. Only Estimator \mathcal{A} is able to consistently produce the next monomial. The above heatmap was constructed through generating 200 circuits for each combination of hyperparameters and computing the corresponding γ_g for each p . This diagram shows the performance when not using the adversarial dataset construction.

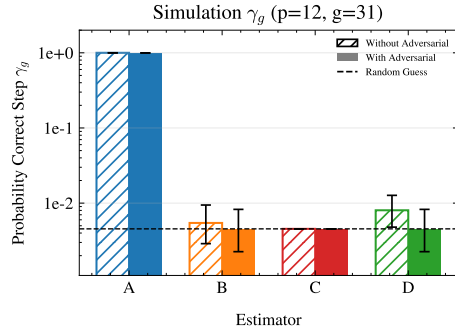


Figure 9: The figure above shows how γ_g changes for Estimators \mathcal{A} , \mathcal{B} , \mathcal{C} , and \mathcal{D} when the data is biased adversarially (as in the results so far) preventing identification monomials from frequency statistics, and without de-biasing.

Table 1: **Likelihood-based fit of LLM accuracy to an effective-prefix model.** Accuracy as a function of prefix length g is fit using two one-parameter models for the effective number of known prefix terms: proportional $k = ug$ and constant-capacity $k = v$. Fits use the binomial log-likelihood aggregated across depths; models are compared via AIC. Reported $\Delta\text{AIC} = \text{AIC}_{\text{constant}} - \text{AIC}_{\text{proportional}}$, so positive values favor proportional scaling. Values $\Delta\text{AIC} < 2$ indicate no meaningful distinction.

Model	u	v	ΔAIC	Better
Qwen3-30B-A3B-Instruct-2507	0.15	0.00	2.21	u
Qwen3-30B-A3B-Thinking-2507	0.47	0.00	228.08	u
Qwen3-4B-Instruct-2507	0.08	0.00	2.32	u
Qwen3-4B-Thinking-2507	0.05	0.00	0.00	–

B The Monomial can be Recovered in Polynomial Time

Given P_g , a solver can form residual labels

$$r^{(k)} := y^{(k)} \oplus \bigoplus_{j=1}^g a_j^{(k)} M_j(v^{(k)}) = M_{g+1}(v^{(k)}), \quad (7)$$

so recovery reduces to identifying the unknown degree- $(d-1)$ support S_{g+1} from labeled payloads.

Let $K_+ := \{k : r^{(k)} = 1\}$ and $T := |K_+|$. Consider the decoder

$$\widehat{S} := \bigcap_{k \in K_+} \text{supp}(v^{(k)}), \quad (8)$$

which outputs \widehat{S} if $T \geq 1$ and $|\widehat{S}| = d-1$, and otherwise declares failure.

Theorem B.1 (Poly-time recovery under fixed-weight payloads). *Fix an instance and assume payloads are i.i.d. uniform on $\{v \in \{0, 1\}^p : \|v\|_0 = w^*\}$ with $w^* \geq d-1$. Let $\rho = \rho(w^*) = \Pr[M_{g+1}(v) = 1]$ and $T = |K_+|$. Then $\Pr[T = 0] = (1 - \rho)^K$. Moreover, conditioned on $T \geq 1$, the decoder succeeds with probability at least*

$$1 - \min \left\{ 1, (p - (d-1)) \left(\frac{w^* - (d-1)}{p - (d-1)} \right)^T \right\}. \quad (9)$$

Proof. If $r^{(k)} = 1$ then $M_{g+1}(v^{(k)}) = 1$, which is equivalent to $S_{g+1} \subseteq \text{supp}(v^{(k)})$. Thus for every $k \in K_+$ we have $S_{g+1} \subseteq \text{supp}(v^{(k)})$, and hence

$$S_{g+1} \subseteq \bigcap_{k \in K_+} \text{supp}(v^{(k)}) = \widehat{S}.$$

Therefore, conditioned on $T \geq 1$, the intersection decoder can fail only if \widehat{S} contains at least one *extraneous* coordinate $i \notin S_{g+1}$, i.e., some $i \in [p] \setminus S_{g+1}$ appears in every positive support.

Fix any $i \notin S_{g+1}$ and consider a single draw v conditioned on $r = 1$ (equivalently, $S_{g+1} \subseteq \text{supp}(v)$). Under the fixed-weight model, after forcing ones on S_{g+1} , the remaining $w^* - (d-1)$ ones are chosen uniformly among the $p - (d-1)$ coordinates in $[p] \setminus S_{g+1}$. Hence

$$\Pr[i \in \text{supp}(v) \mid r = 1] = \frac{w^* - (d-1)}{p - (d-1)}.$$

Now condition on the event $\{T = |K_+|\}$ and on the index set K_+ itself. Because the original examples are i.i.d., the payloads $\{v^{(k)}\}_{k \in K_+}$ are i.i.d. draws from the conditional distribution $(v \mid r = 1)$, so

$$\Pr \left[i \in \text{supp}(v^{(k)}) \ \forall k \in K_+ \mid T \right] = \left(\frac{w^* - (d-1)}{p - (d-1)} \right)^T.$$

Taking a union bound over the $p - (d-1)$ possible extr coordinates gives

$$\Pr[\widehat{S} \neq S_{g+1} \mid T] \leq (p - (d-1)) \left(\frac{w^* - (d-1)}{p - (d-1)} \right)^T,$$

which implies (9). Finally, since $T = \sum_{k=1}^K \mathbf{1}\{r^{(k)} = 1\}$ with $\Pr[r^{(k)} = 1] = \rho = \rho(w^*)$, we have $\Pr[T = 0] = (1 - \rho)^K$. \square

Corollary B.2 (High-probability recovery with K samples). *In the setting of Thm. B.1, let $\rho := \rho(w^*) = \Pr[M_{g+1}(v) = 1]$ and $\alpha := \frac{w^* - (d-1)}{p - (d-1)} \in [0, 1)$. Fix $\delta \in (0, 1)$. For $\alpha \in (0, 1)$ define*

$$T_0 := \left\lceil \frac{\log(2(p - (d-1))/\delta)}{\log(1/\alpha)} \right\rceil \quad (\text{and if } \alpha = 0, \text{ take } T_0 := 1).$$

If $K \geq \frac{1}{\rho} \max\{2T_0, 8 \log(2/\delta)\}$, then the decoder in (8) outputs $\widehat{S} = S_{g+1}$ with probability at least $1 - \delta$.

Proof. Let $T = |K_+| = \sum_{k=1}^K \mathbf{1}\{r^{(k)} = 1\}$. Since $r^{(k)} = M_{g+1}(v^{(k)})$ and the payloads are i.i.d., we have $T \sim \text{Bin}(K, \rho)$.

By Thm. B.1, for any $t \geq 1$,

$$\Pr[\widehat{S} \neq S_{g+1} \mid T = t] \leq (p - (d-1))\alpha^t.$$

Hence

$$\Pr[\widehat{S} \neq S_{g+1}] \leq \Pr[T < T_0] + \Pr[\widehat{S} \neq S_{g+1} \mid T \geq T_0].$$

For the first term, our lower bound on K implies $K\rho/2 \geq T_0$, so by a multiplicative Chernoff bound,

$$\Pr[T < T_0] \leq \Pr\left[T \leq \frac{1}{2}K\rho\right] \leq \exp\left(-\frac{1}{8}K\rho\right) \leq \delta/2,$$

where the last inequality uses $K\rho \geq 8\log(2/\delta)$.

For the second term, on $T \geq T_0$ we have

$$\Pr[\widehat{S} \neq S_{g+1} \mid T \geq T_0] \leq (p - (d - 1))\alpha^{T_0} \leq \delta/2,$$

by the definition of T_0 (and trivially if $\alpha = 0$). Combining the two bounds yields $\Pr[\widehat{S} \neq S_{g+1}] \leq \delta$. \square

Lem. 4.3 shows a *per-sample* obfuscation property: marginalizing over the unknown prefix supports, each labeled example provides only exponentially small Bayes advantage about the next-term signal unless one conditions on the revealed prefix. In the ideal balanced case $\rho(w^*) = 1/2$, this advantage is 0 whenever $m(a) \geq 1$. While the trivial leakage case $m(a) = 0$ is theoretically possible, its probability 2^{-g} becomes exponentially rare as depth increases. Lem. 4.1 rules out history-only shortcuts under the instance distribution, since S_{g+1} remains uniform given the revealed prefix.

Finally, Thm. B.1 (and Corollary B.2) show that a diligent solver can subtract the prefix mask to obtain residual labels $r^{(k)} = M_{g+1}(v^{(k)})$ and recover t_{g+1} in polynomial time from $K = O(\frac{1}{\rho(w^*)} \log(p/\delta))$ samples with failure probability at most δ (for fixed d and constant $\rho(w^*)$). Together, these properties justify using γ_g in (4) as an operational measure of step success in our benchmark.

Efficient validation. Given the instance specification (in particular S_{g+1}) and a candidate monomial \tilde{t} , the validator parses \tilde{t} , rejects unless it contains exactly one address variable (which must be a_{g+1}) and exactly $d - 1$ distinct payload variables, then accepts iff the parsed payload index set \tilde{S} equals S_{g+1} . This runs in time $O(|\tilde{t}| + d \log d)$ worst-case (or $O(|\tilde{t}| + d)$ expected with hashing).